

OILSAM2: MEMORY-AUGMENTED SAM2 FOR SCALABLE SAR OIL SPILL DETECTION

Shuaiyu Chen¹, Ming Yin¹, Peng Ren², Chunbo Luo³, Zeyu Fu^{1*}

¹ Multimodal Intelligence Lab, Department of Computer Science, University of Exeter, United Kingdom

² College of Oceanography and Space Informatics, China University of Petroleum (East China), China.

³ Department of Computer Science, University of Exeter, United Kingdom

ABSTRACT

Segmenting oil spills from Synthetic Aperture Radar (SAR) imagery remains challenging due to severe appearance variability, scale heterogeneity, and the absence of temporal continuity in real-world monitoring scenarios. While foundation models such as Segment Anything (SAM) enable prompt-driven segmentation, existing SAM-based approaches operate on single images and cannot effectively reuse information across scenes. Memory-augmented variants (e.g., SAM2) further assume temporal coherence, making them prone to semantic drift when applied to unordered SAR image collections. We propose OilSAM2, a memory-augmented segmentation framework tailored for unordered SAR oil spill monitoring. OilSAM2 introduces a hierarchical feature-aware multi-scale memory bank that explicitly models texture-, structure-, and semantic-level representations, enabling robust cross-image information reuse. To mitigate memory drift, we further propose a structure–semantic consistent memory update strategy that selectively refreshes memory based on semantic discrepancy and structural variation. Experiments on two public SAR oil spill datasets demonstrate that OilSAM2 achieves state-of-the-art segmentation performance, delivering stable and accurate results under noisy SAR monitoring scenarios. The source code is available at <https://github.com/Chenshuaiyu1120/OILSAM2>.

Index Terms— Oil Spill Detection, Synthetic Aperture Radar, Segment Anything Model 2

1. INTRODUCTION

Marine oil spills caused by offshore drilling accidents [1], pipeline failures [2], and tanker incidents [3] pose serious threats to marine ecosystems and coastal regions, so reliable identification of oil-contaminated areas is important for environmental monitoring and emergency response [4]. Synthetic aperture radar (SAR) has become a primary data source for oil spill monitoring because it operates independently of weather conditions and daylight [5]. With the increasing availability of large-scale SAR Earth observation data, deep learning-based methods have emerged as an effective solution for automatic oil spill detection [5–7].

Convolutional neural network (CNN)-based approaches [8–12] have demonstrated superior performance and robustness in SAR-based oil spill detection, outperforming traditional thresholding and handcrafted feature-based methods [10, 13–16] by learning discriminative representations directly from data. In addition, Transformer-based models [17, 18] use self-attention to model relationships among all image patches at the same time, so global contextual information can be captured directly for segmentation [11]. However,

self-attention introduces high computational cost, which limits the use of transformers in large-scale SAR oil spill monitoring [11, 17]. To reduce this burden, recent work has explored sequence modeling approaches based on state-space models (SSMs), which support long-range dependency modeling with linear computational complexity. Based on this idea, OSDMamba [19] proposes a Mamba-based architecture for SAR oil spill segmentation. By using selective state-space scanning, OSDMamba captures long-range dependencies and global context while keeping computation efficient.

Recently, foundation models such as the Segment Anything Model (SAM) [20] have demonstrated the potential of adapting SAM through domain-specific prompt fusion [21]. However, SAM-based approaches operate on single images and cannot reuse information across scenes, which is often desirable in operational settings where SAR data are processed as collections rather than isolated samples. To address this, SAM2 [22] introduces a memory mechanism for cross-image information reuse, though it has not yet been explored for SAR oil spill detection.

Adapting memory-based SAM frameworks to oil spill monitoring poses two main challenges. 1) Oil spills exhibit heterogeneous cues across feature scales, from fine-grained texture and speckle to higher-level structural and semantic representations, which a single-scale memory cannot capture effectively. 2) SAR oil spill images are unordered and lack temporal continuity, making memory retrieval sensitive to scene-specific variations such as sea state, backscatter intensity, and speckle noise, which can lead to the propagation of irrelevant information. These challenges motivate a structured and task-adaptive memory design for unordered SAR oil spill segmentation.

In this paper, we propose OilSAM2, a SAM2-based architecture tailored for SAR oil spill segmentation, as illustrated in Fig. 1. OilSAM2 is built on a memory-based SAM framework [23] by introducing a hierarchical feature-aware memory bank that explicitly models texture-, structure-, and semantic-level representations. To accommodate the unordered nature of SAR imagery and mitigate semantic drift, we further propose a structure–semantic consistent memory update strategy that regulates memory refreshing using reliability cues. This design enables robust cross-image information reuse while preserving compatibility with the original SAM interaction paradigm. Extensive experiments on two publicly available SAR oil spill datasets demonstrate that OilSAM2 achieves strong segmentation performance and improved robustness under diverse imaging and environmental conditions.

*Corresponding Author.

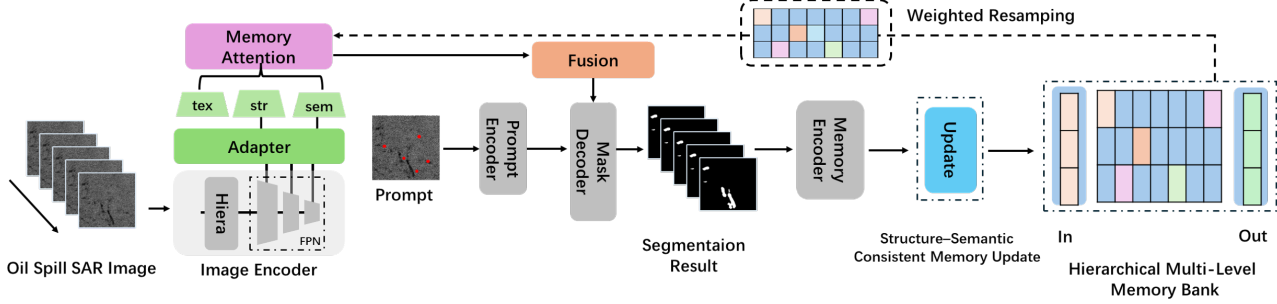


Fig. 1. Overview of the proposed OilsAM2 framework. Given an input SAR image and user prompt, hierarchical features are extracted and organized into texture-, structure-, and semantic-level representations. Each level interacts with a corresponding memory group via scale-wise attention. The retrieved features are adaptively fused and decoded to produce the segmentation mask, while a structure–semantic consistent update strategy regulates memory refreshing for robust reuse across unordered SAR images.

2. METHOD

2.1. Problem Formulation

We study prompt-driven SAR oil spill segmentation over an unordered image collection $\mathcal{X} = \{x_t\}_{t=1}^T$, where the index t denotes the processing order rather than chronological time. Given an input SAR image $x_t \in \mathbb{R}^{H \times W}$ and a user prompt p (e.g., clicks or bounding boxes), the goal is to predict a pixel-wise segmentation mask. We denote the number of semantic classes by C (with $C=2$ for binary oil-spill segmentation). The ground-truth label map is $y_t \in \{0, 1, \dots, C-1\}^{H \times W}$, and the model produces a soft prediction $\hat{Y}_t \in [0, 1]^{C \times H \times W}$, where $\sum_{c=0}^{C-1} \hat{Y}_t(c, x, y) = 1$ for each pixel (x, y) . The final hard mask is $\hat{y}_t(x, y) = \arg \max_c \hat{Y}_t(c, x, y)$.

Following the general formulation in [23], each image x_t is encoded by an image encoder E_{img} to obtain visual features $F_t = E_{\text{img}}(x_t)$, while the prompt p is mapped to a prompt embedding $Q = E_{\text{prompt}}(p)$ via a prompt encoder E_{prompt} . A memory bank $\mathcal{M}_{t-1} = \{(K_j, V_j)\}$ maintains a compact set of key–value representations derived from previously processed images, where K_j denotes a memory key and V_j is the associated value used for segmentation guidance.

Given the current features F_t , a subset of memory entries $\tilde{\mathcal{M}}_{t-1} \subseteq \mathcal{M}_{t-1}$ is retrieved based on feature similarity and fused with the image features and prompt embedding through a memory attention module $A(\cdot)$. The aggregated representation is decoded by a mask decoder $D(\cdot)$ to yield the per-pixel class probabilities:

$$\hat{Y}_t = \text{Softmax}\left(D\left(A\left(F_t, \tilde{\mathcal{M}}_{t-1}, Q\right)\right)\right). \quad (1)$$

After prediction, the model encodes the output (e.g., \hat{Y}_t or \hat{y}_t together with F_t) via a memory encoder to form a new memory entry, which is inserted into the memory bank. The memory bank is periodically updated to retain a compact and representative set of entries.

While this formulation provides an effective baseline for SAR oil spill segmentation, it does not explicitly account for the unordered nature of SAR imagery or the multi-level feature heterogeneity of oil spills. These limitations motivate the structured memory design and update strategies introduced in the following sections.

2.2. Hierarchical Feature-Aware Memory Bank

SAR oil spill appearance varies across feature abstraction levels. Fine-grained texture and speckle statistics are essential for detecting fragmented slicks, mid-level structural patterns capture elongated

morphology, and higher-level semantic representations help suppress visually similar look-alike phenomena. Encoding these heterogeneous cues within a single memory space can blur level-specific information and degrade retrieval reliability. As illustrated in Fig. 1, our framework exploits the hierarchical representations produced by modern image encoders to construct a structured multi-level memory bank. Modern image encoders [22, 23] naturally produce hierarchical feature representations at different depths. Given an input x_t , we denote the resulting features as $\{F_t^{(s)}\}_{s \in \{\text{tex}, \text{str}, \text{sem}\}}$, corresponding to early-, middle-, and late-stage encoder outputs. Leveraging this hierarchy, we construct a structured multi-level memory bank that explicitly stores complementary information at three feature levels: texture (tex), structure (str), and semantic (sem). The memory at step $t-1$ is defined as

$$\mathcal{M}_{t-1} = \{\mathcal{M}_{t-1}^{\text{tex}}, \mathcal{M}_{t-1}^{\text{str}}, \mathcal{M}_{t-1}^{\text{sem}}\}, \quad (2)$$

where each group contains key–value pairs

$$\mathcal{M}_{t-1}^{(s)} = \{(K_j^{(s)}, V_j^{(s)})\}_{j=1}^{N_s}, \quad s \in \{\text{tex}, \text{str}, \text{sem}\}. \quad (3)$$

Each feature level interacts exclusively with its corresponding memory group, preserving level-specific representations and improving robustness under diverse SAR imaging conditions.

2.3. Scale-Adaptive Memory Fusion

Although the multi-level memory bank supports structured information reuse, features retrieved from different levels are heterogeneous and may contribute unequally across oil spill morphologies and sea states. We therefore introduce a scale-adaptive fusion module to integrate complementary information across feature levels.

Memory retrieval is performed independently at each level. For $s \in \{\text{tex}, \text{str}, \text{sem}\}$, the feature $F_t^{(s)}$ is first mapped into a shared embedding space via a lightweight adapter, followed by scale-wise memory attention to obtain

$$\tilde{F}_t^{(s)} = A\left(F_t^{(s)}, \mathcal{M}_{t-1}^{(s)}, Q_t\right), \quad (4)$$

where $\tilde{\mathcal{M}}_{t-1}^{(s)}$ denotes the retrieved memory entries at level s .

We then align $\{\tilde{F}_t^{(s)}\}$ to the same spatial resolution and compute a level-wise response score

$$e_t^{(s)} = \|\tilde{F}_t^{(s)}\|_1, \quad (5)$$

Table 1. Comparison of OilSAM2 with other oil spill segmentation methods on the M4D Dataset [24].

Model	SeaSurface(% , \uparrow)	Oil Spill(% , \uparrow)	Look-alike(% , \uparrow)	Ship(% , \uparrow)	Land(% , \uparrow)	mIoU(% , \uparrow)
Unet [25]	93.90	53.79	39.55	44.93	92.68	64.97
LinkNet [26]	94.99	51.53	43.24	40.23	93.97	64.79
PSPNet [27]	92.78	40.10	33.79	24.42	86.90	55.60
Deeplabv2 [28]	94.09	25.57	40.30	11.41	74.99	49.27
Deeplabv2(msc) [28]	95.39	49.28	31.26	88.65	93.97	62.83
Deeplabv3+ [29]	96.43	53.38	55.40	27.63	92.44	65.06
TransOilSeg [11]	97.02	61.38	62.41	33.49	94.39	69.74
YOLOv8-SAM [21]	94.34	41.84	48.15	52.48	87.65	64.89
SAM-OIL [21]	96.05	51.60	55.60	52.55	91.81	69.52
OSDMamba [19]	96.47	65.59	47.57	46.85	94.76	70.25
OilSAM2(Ours)	95.10	65.92	54.16	56.18	92.07	72.62

which serves as a lightweight indicator of the contribution of level s for the current input. The scores are normalized to obtain fusion weights

$$\gamma_t^{(s)} = \frac{\exp(e_t^{(s)})}{\sum_{s' \in \{\text{tex}, \text{str}, \text{sem}\}} \exp(e_t^{(s')})}. \quad (6)$$

Finally, the fused representation is computed as

$$F_t^* = \sum_{s \in \{\text{tex}, \text{str}, \text{sem}\}} \gamma_t^{(s)} \tilde{F}_t^{(s)}, \quad (7)$$

which is forwarded to the mask decoder for final segmentation prediction.

2.4. Structure-Semantic Consistent Memory Update

Sections 2.2 and 2.3 describe how OilSAM2 retrieves and fuses multi-level memory for mask prediction. We now introduce a structure-semantic consistent memory update strategy. Unlike temporally coherent settings [23], our SAR inputs are unordered; thus, updating memory after every prediction can accumulate scene-specific artifacts (e.g., sea state and speckle), which are later retrieved and cause semantic drift.

To regulate memory refreshing, we maintain lightweight structure/semantic prototypes, $F_{\text{mem}}^{\text{str}}$ and $z_{\text{mem}}^{\text{sem}}$, summarizing the current memory state. For the current sample, we extract a semantic descriptor

$$z_t^{\text{sem}} = \text{GAP}(F_t^{\text{sem}}), \quad (8)$$

and measure semantic discrepancy via cosine distance

$$\Delta_{\text{sem}} = 1 - \cos(z_t^{\text{sem}}, z_{\text{mem}}^{\text{sem}}). \quad (9)$$

At the structure level, we measure boundary variation using gradient magnitude

$$\Delta_{\text{str}} = \frac{1}{HW} \|\nabla F_t^{\text{str}} - \nabla F_{\text{mem}}^{\text{str}}\|_1. \quad (10)$$

where H and W denote the spatial height and width of the feature maps.

We update semantic memory when $\Delta_{\text{sem}} > \tau_{\text{sem}}$ and structure memory when $\Delta_{\text{str}} > \tau_{\text{str}}$; the texture group is refreshed only together with a semantic or structural update to preserve cross-level consistency. When triggered, new memory content $M_t^{(s)}$ is encoded from the current sample and integrated via exponential moving average:

$$M_{\text{mem}}^{(s)} \leftarrow (1 - \alpha) M_{\text{mem}}^{(s)} + \alpha M_t^{(s)}, \quad (11)$$

where α controls the update rate, limiting abrupt shifts under noisy SAR conditions.

3. EXPERIMENTS

3.1. Datasets

We conduct experiments on two widely used SAR oil spill Datasets: the M4D dataset [24] and the Deep-SAR Oil Spill (SOS) dataset the [30]. The M4D dataset [24] consists of 1,002 training and 110 testing SAR images with a resolution of 1250×650 pixels, covering five semantic categories: sea surface, oil spill, look-alike phenomena, ships, and land.

The SOS dataset [30] contains 8,070 labeled SAR image patches (256×256 pixels) derived from ALOS PALSAR and Sentinel-1A imagery over the Gulf of Mexico and Persian Gulf. It is split into 6,455 training and 1,615 testing samples, covering diverse sea states and spill morphologies for robust oil spill detection.

3.2. Implementation Details

Our framework is implemented in PyTorch and trained on a single NVIDIA L40 GPU. The AdamW optimizer is adopted with an initial learning rate of 0.001, weight decay of 0.0001, and batch size of 4. The model is trained using a weighted binary cross-entropy loss, following the setting used in [23]. During training, the image encoder, prompt encoder, and the original memory attention and memory encoder modules of SAM2 [22] are kept frozen. The proposed scale adapters, multi-scale memory components, and structure-semantic update modules are trained together with the SAM mask decoder.

3.3. Comparison with State-of-the-Art

Table 1 presents quantitative results compared with classical CNN-based (U-Net [25], PSPNet [27], DeepLabv3+ [29]), transformer-based, and SAM-derived methods. Our method achieves consistent improvements across both the M4D [24] and SOS datasets. On the M4D dataset (Table 1), our approach obtains a 14.32% increase in Oil Spill IoU and a 3.10% increase in overall mIoU compared to SAM-Oil, demonstrating the effectiveness of memory-augmented segmentation in handling complex spill morphologies. Notably, OilSAM2 not only improves the detection of oil spills but also maintains competitive performance across other semantic categories such as look-alikes, ships, and land, indicating better generalization to diverse marine targets.

On the SOS dataset (Table 2), the proposed framework outperforms classical CNN-based models such as U-Net and D-LinkNet, advanced segmentation networks including DeepLabv3 and CBD-Net, and foundation-model-based approaches such as SAM2. Oil-

Table 2. Comparison of OilSAM2 with other oil spill segmentation methods (on SOS Dataset [30]).

Model	mIoU (% , \uparrow)		F1-score (% , \uparrow)		Recall (% , \uparrow)		Precision (% , \uparrow)	
	PALSAR	Sentinel-1	PALSAR	Sentinel-1	PALSAR	Sentinel-1	PALSAR	Sentinel-1
U-Net [25]	81.63	81.46	82.20	86.10	77.84	81.22	83.08	85.61
D-LinkNet [26]	81.58	82.32	84.57	87.08	85.48	85.22	83.69	85.22
Deeplabv3 [29]	81.79	82.94	84.26	87.70	84.31	84.76	83.02	88.08
CBD-Net [30]	83.31	83.42	84.84	87.87	86.75	87.32	84.20	91.20
Medical SAM2 [23]	82.14	80.64	83.04	82.13	83.77	85.92	81.07	85.64
TransOilSeg	83.08	82.27	96.73	93.18	96.52	93.07	96.94	93.43
OilSAM2 (Ours)	84.20	83.67	83.98	88.75	87.64	86.51	83.58	90.39

Table 3. Ablation study of components (SOS Dataset PALSAR). Scale adapters are replaced by linear projections in the ablation study.

Configuration	mIoU	Prec.
Baseline [23]	82.14	81.07
Baseline + Multi-Scale Fusion	82.27	81.13
Baseline + Structure–Semantic Update	83.64	81.68
Baseline + Multi-scale Memory Bank	83.53	82.04
Baseline + Fusion + Update	83.92	82.16
Baseline + Fusion + Memory Bank	83.85	82.24
Baseline + Update + Memory Bank	84.10	83.06
OILSAM2 (Full Model)	84.20	83.58

SAM2 achieves the highest mIoU of 84.20% on PALSAR and 83.67% on Sentinel-1, and it also shows a higher F1-score and recall. These results show that the structure–semantic consistent update helps stabilize boundary delineation, the multi-scale memory bank captures oil slicks at different scales, and the multi-scale fusion strategy supports adaptive aggregation of complementary representations.

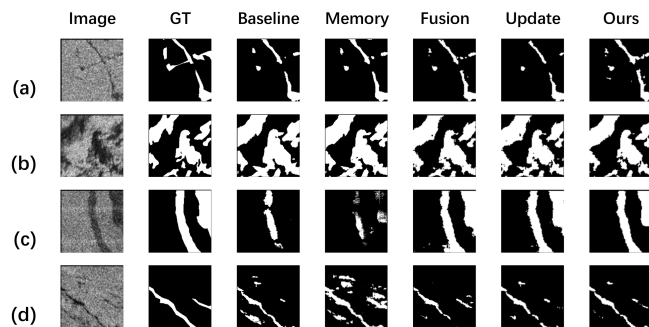
3.4. Ablation Study

To evaluate the contribution of each proposed component, we conduct an ablation study on the SOS dataset. Quantitative results are reported in Table 3, and qualitative comparisons are shown in Figure 2.

Starting from the baseline model [23], we examine each component separately. Adding the multi-scale fusion strategy alone results in a small improvement, which indicates that adaptive feature aggregation provides limited benefit when memory augmentation is not used. Adding the structure–semantic consistent update produces a larger gain in both mIoU and precision. This result suggests that updating memory based on semantic and structural cues helps stabilize memory evolution and preserve boundary information. Introducing the multi-scale memory bank alone also leads to a clear performance improvement, which confirms that organizing memory across texture, structure, and semantic levels is effective.

We then study the combined effects of different components. As shown in Table 3, combining the structure–semantic update with the multi-scale memory bank yields the largest gain among all two-component variants. This result reflects a strong interaction between structured memory representation and controlled memory updating. Combining the fusion strategy with either component also improves performance, but the gains are smaller.

When all components are included, the full OilSAM2 model achieves the best performance across all metrics. The results indi-

**Fig. 2.** Qualitative results of the ablation study (On SOS Dataset).

cate that the three components complement each other. Multi-scale fusion aggregates information across different representation levels, the multi-scale memory bank captures heterogeneous spatial patterns, and the structure–semantic update maintains stable memory evolution.

Qualitative results in Figure 2 are consistent with the quantitative analysis. Compared with reduced variants, the full model produces clearer boundaries, improves detection of small and fragmented oil slicks, and reduces missed and false detections under complex sea conditions.

4. CONCLUSION

In this paper, we presented OilSAM2, a memory-augmented segmentation framework for unordered SAR oil spill monitoring. OilSAM2 extends SAM2 with a hierarchical feature-aware multi-scale memory bank and a structure–semantic consistent memory update strategy, enabling robust cross-image information reuse under diverse SAR imaging conditions. The multi-scale memory design captures complementary texture-, structure-, and semantic-level representations, supporting accurate segmentation of both fragmented and large-scale oil spills, while the proposed update mechanism prevents semantic drift by regulating memory refreshing based on reliability cues. Experimental results on benchmark SAR datasets demonstrate that OilSAM2 consistently outperforms CNN-based, transformer-based, and SAM-derived baselines, providing improved robustness and cross-image consistency for effective oil spill monitoring.

5. REFERENCES

- [1] A. P. Bentz, “Oil spill identification,” *Analytical Chemistry*, vol. 48, no. 6, pp. 454A–472A, 1976.

- [2] J. W. Doerffer, *Oil spill response in the marine environment*, Elsevier, 2013.
- [3] R. Al-Ruzouq, M. B. A. Gibril, A. Shanableh, et al., “Sensors, features, and machine learning for oil spill detection and monitoring: A review,” *Remote Sensing*, vol. 12, no. 20, pp. 3338, 2020.
- [4] A. H. S. Solberg, C. Brekke, and P. O. Husoy, “Oil spill detection in radarsat and envisat sar images,” *IEEE Transactions on Geoscience and Remote Sensing*, vol. 45, no. 3, pp. 746–755, 2007.
- [5] C. Brekke and A. H. S. Solberg, “Oil spill detection by satellite remote sensing,” *Remote Sensing of Environment*, vol. 95, no. 1, pp. 1–13, 2005.
- [6] A. R. Satyanarayana and M. A. Dhali, “Oil spill segmentation using deep encoder-decoder models,” 2023.
- [7] K. Kikaki, I. Kakogeorgiou, I. Hoteit, et al., “Detecting marine pollutants and sea surface features with deep learning in sentinel-2 imagery,” *ISPRS Journal of Photogrammetry and Remote Sensing*, vol. 210, pp. 39–54, 2024.
- [8] A. R. Satyanarayana and M. A. Dhali, “Oil spill segmentation using deep encoder-decoder models,” 2023.
- [9] O. Ronneberger, P. Fischer, and T. Brox, “U-net: Convolutional networks for biomedical image segmentation,” in *Medical Image Computing and Computer-Assisted Intervention—MICCAI 2015*. Springer, 2015, pp. 234–241.
- [10] C. Li, M. Wang, X. Yang, and D. Chu, “Ds-unet: Dual-stream u-net for oil spill detection of sar image,” *IEEE Geoscience and Remote Sensing Letters*, vol. 20, pp. 1–5, 2023.
- [11] Yu et al, “Transoilseg: A novel sar oil spill detection method addressing data limitations and look-alike confusions,” *IEEE Transactions on Geoscience and Remote Sensing*, 2025.
- [12] Shuaiyu Chen, Chunbo Luo, Peng Ren, and Zeyu Fu, “Enhancing marine pollution detection in remote sensing via self-supervised boundary awareness,” in *Proceedings of the British Machine Vision Conference (BMVC)*, 2025.
- [13] Fiscella et al, “Oil spill detection using marine sar images,” *International Journal of Remote Sensing*, vol. 21, no. 18, pp. 3561–3566, 2000.
- [14] Y. Guo and H. Z. Zhang, “Oil spill detection using synthetic aperture radar images and feature selection in shape space,” *International Journal of Applied Earth Observation and Geoinformation*, vol. 30, pp. 146–157, 2014.
- [15] S. Temitope Yekeen and A.-L. Balogun, “Advances in remote sensing technology, machine learning and deep learning for marine oil spill detection, prediction and vulnerability assessment,” *Remote Sensing*, vol. 12, no. 20, pp. 3416, 2020.
- [16] S. Dehghani-Dehcheshmeh, M. Akhoondzadeh, and S. Homayouni, “Oil spills detection from sar earth observations based on a hybrid cnn transformer networks,” *Marine Pollution Bulletin*, vol. 190, pp. 114834, 2023.
- [17] Dehghani et al, “Oil spills detection from sar earth observations based on a hybrid cnn transformer networks,” *Marine Pollution Bulletin*, vol. 190, pp. 114834, 2023.
- [18] J. Kang, C. Yang, J. Yi, et al., “Detection of marine oil spill from planetscope images using cnn and transformer models,” *Journal of Marine Science and Engineering*, vol. 12, no. 11, pp. 2095, 2024.
- [19] Shuaiyu Chen, Fu Wang, Peng Ren, Chunbo Luo, and Zeyu Fu, “Osdmamba: Enhancing oil spill detection from remote sensing images using selective state space model,” *IEEE Geoscience and Remote Sensing Letters*, 2025.
- [20] Alexander Kirillov, Eric Mintun, Nikhila Ravi, Hanzi Mao, Chloe Rolland, Laura Gustafson, Tete Xiao, Spencer Whitehead, Alexander C Berg, Wan-Yen Lo, et al., “Segment anything,” in *Proceedings of the IEEE/CVF international conference on computer vision*, 2023, pp. 4015–4026.
- [21] W. Wu, M. S. Wong, X. Yu, G. Shi, C. Y. T. Kwok, and K. Zou, “Compositional oil spill detection based on object detector and adapted segment anything model from sar images,” *IEEE Geoscience and Remote Sensing Letters*, 2024.
- [22] Nikhila Ravi et al, “Sam 2: Segment anything in images and videos,” 2024.
- [23] Jiayuan Zhu, Abdullah Hamdi, Yunli Qi, Yueming Jin, and Junde Wu, “Medical sam 2: Segment medical images as video via segment anything model 2,” 2024.
- [24] Marios Krestenitis, Georgios Orfanidis, Konstantinos Ioannidis, Konstantinos Avgerinakis, Stefanos Vrochidis, and Ioannis Kompatsiaris, “Oil spill identification from satellite images using deep neural networks,” *Remote Sensing*, vol. 11, no. 15, pp. 1762, 2019.
- [25] O. Ronneberger, P. Fischer, and T. Brox, “U-net: Convolutional networks for biomedical image segmentation,” in *MICCAI*. Springer, 2015, pp. 234–241.
- [26] A. Chaurasia and E. Culurciello, “Linknet: Exploiting encoder representations for efficient semantic segmentation,” in *2017 IEEE Visual Communications and Image Processing (VCIP)*. IEEE, 2017, pp. 1–4.
- [27] H. Zhao, J. Shi, X. Qi, et al., “Pyramid scene parsing network,” in *Proceedings of the IEEE Conference on Computer Vision and Pattern Recognition*, 2017, pp. 2881–2890.
- [28] L. C. Chen, G. Papandreou, I. Kokkinos, et al., “Deeplab: Semantic image segmentation with deep convolutional nets, atrous convolution, and fully connected crfs,” *IEEE Transactions on Pattern Analysis and Machine Intelligence*, vol. 40, no. 4, pp. 834–848, 2017.
- [29] L. C. Chen, Y. Zhu, G. Papandreou, et al., “Encoder-decoder with atrous separable convolution for semantic image segmentation,” in *Proceedings of the European Conference on Computer Vision (ECCV)*, 2018, pp. 801–818.
- [30] Zhu et al, “Oil spill contextual and boundary-supervised detection network based on marine sar images,” *IEEE Transactions on Geoscience and Remote Sensing*, vol. 60, pp. 1–10, 2022.